Insulator at the Ultrathin Limit: MgO on Ag(001)

Silvia Schintke,[1] Stéphane Messerli,[1] Marina Pivetta,[1] François Patthey,[1] Laurent Libioulle,[1] Massimiliano Stengel,[2] Alessandro De Vita,[2,3] and Wolf-Dieter Schneider[1]

[1]*Institut de Physique de la Matière Condensée, Université de Lausanne, CH-1015 Lausanne, Switzerland*
[2]*Institut Romand de Recherche Numérique en Physique des Matériaux, PHH-Ecublens, CH-1015 Lausanne, Switzerland*
[3]*INFM and Dipartimento di Ingegneria dei Materiali, Università di Trieste, via A. Valerio 2, 34127 Trieste, Italy*

(Received 21 January 2000; revised manuscript received 27 February 2001; published 7 December 2001)

The electronic structure and morphology of ultrathin MgO films epitaxially grown on Ag(001) were investigated using low-temperature scanning tunneling spectroscopy and scanning tunneling microscopy. Layer-resolved differential conductance (dI/dU) measurements reveal that, even at a film thickness of three monolayers, a band gap of about 6 eV is formed corresponding to that of the MgO(001) single-crystal surface. This finding is confirmed by layer-resolved calculations of the local density of states based on density functional theory.

DOI: 10.1103/PhysRevLett.87.276801 PACS numbers: 73.20.At, 68.37.Ef, 77.55.+f, 79.60.Bm

Insulators like many metal oxides are of considerable technological importance, e.g., as insulating barriers in miniaturized electronic circuits, as magnetic tunnel junctions [1] in magnetoelectronics and magnetic data storage, or for the development of a variety of nanodevices based on oxide heterostructures. Intensive surface science studies have been performed on single crystal metal oxide surfaces [2,3] and thin films [4–6] in order to understand their surface structure and their electronic properties on a microscopic level. The band structure of wide band gap materials might be strongly modified when their size is varied from the molecular regime to macroscopic crystals [7], thus influencing electronic and dielectric properties, as well as the chemical reactivities at the surface. Therefore, it is of fundamental interest to explore the changes of the surface electronic structure with respect to layer thickness until the electronic structure of a macroscopic single crystal surface is achieved.

Recently, the growth of ultrathin insulating NaCl layers on Al(111) [8] and of CoO and NiO layers on Ag(001) [9] has been studied by scanning tunneling microscopy (STM) and atomic resolution has been obtained. From the change in image contrast a maximum thickness of three layers for successful imaging was inferred [8]. Based on image contrast as well as on tunneling current versus voltage curves taken on both NiO islands and Ag substrate, the existence of a band gap has been deduced [9]. For nanostructures of CaF_1 and CaF_2 on Si(111), chemical imaging of insulators has been demonstrated using scanning tunneling spectroscopy (STS) in combination with a simple model for tunneling across two barriers, the vacuum gap and the insulating film [10]. However, no atomic resolution has been obtained in this case and, for CaF_2, it is only assumed that the full gap is already formed for the first CaF layer on Si(111) [10].

In this Letter, we determine for the first time layer-by-layer the electronic structure and the morphology of ultrathin MgO films on Ag(001) by STS and STM measurements and by *ab initio* calculations of the local density of states (LDOS) using density functional theory (DFT). We show that the electronic structure of the corresponding insulator crystal surface already forms within the first three monolayers (ML).

The experiments were performed with a homebuilt low-temperature STM in ultrahigh vacuum [11]. The single crystal Ag(001) surface was cleaned by standard sputtering and annealing. Epitaxial MgO films were grown on a Ag(001) substrate at 500 K by evaporating Mg in an O_2 partial pressure of 1×10^{-6} mbar [12]. Stoichiometry and 1×1 surface crystalline structure of MgO(001) films were cross-checked by Auger electron spectroscopy, x-ray photoelectron spectroscopy, and low energy electron diffraction. Ultrathin MgO films (0.3–5 ML) were studied with STM and STS at 50 K. Differential conductance spectra (dI/dU), related to the LDOS [13], were measured with lock-in detection (270 Hz sinusoidal modulation of 5 mV amplitude added to the bias). All features of the spectra were carefully checked for reproducibility with different tunnel currents, tip-sample distances, and tip conditions, and on various topographically comparable surface regions. For acquiring dI/dU spectra over wide voltage intervals, the tip-sample separation z was varied during the voltage sweep in different modes, i.e., by a linear ramp ($dz/dU = \text{const}$) [14], or by keeping constant either the tunnel current or the tunnel resistance [15,16]. For comparison, electron energy loss spectroscopy (EELS) and angle-resolved ($\pm 2°$) ultraviolet photoelectron spectroscopy (UPS) were performed [17].

Figure 1 shows STM images displaying typical surface geometries used for dI/dU measurements. After deposition of 0.3 ML MgO (Fig. 1a) two-dimensional square islands of 10–15 nm size have nucleated homogeneously on the Ag(001) surface. Some islands near a silver step edge are embedded in the silver layer of the upper terrace, due to Ag adatom diffusion at elevated sample temperature [18]. Thus, the two different island contrasts (i), (ii) near a terrace step (Fig. 1a) are indicative of the position and [100] orientation of the terrace step prior to nucleation.

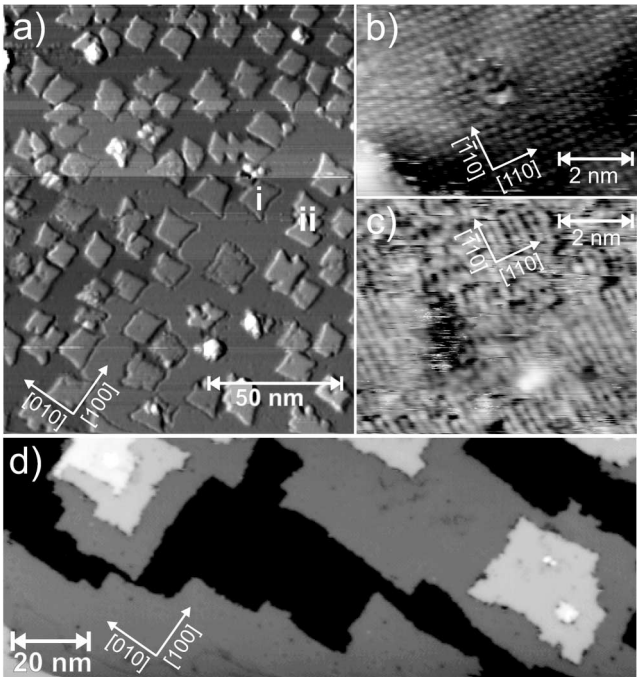

FIG. 1. STM images of (a) 0.3 ML MgO/Ag(001), $U = 5.0$ V, $I = 1.0$ nA; (b) Ag(001) atomic resolution *through* an MgO island, $U = 30$ mV, $I = 2$ pA (left bottom corner: bare Ag substrate); (c) atomic resolution of the MgO layer (one type of ion is resolved), $U = 2.5$ V, $I = 50$ pA; (d) 2.0 ML MgO/Ag(001), $U = 3.0$ V, $I = 1.0$ nA.

After deposition of about 2 ML MgO (Fig. 1d) the Ag surface is completely covered with MgO, forming terraces of typically 50 nm width and 3D pyramidic islands which allow layer dependent dI/dU measurements. The typical surface density of point defects in these films is $<0.1\%$ of a ML [19].

Figure 2a shows representative dI/dU spectra measured with the tip positioned above a 1 ML thick MgO island (free of defects on a scale of 10 nm $\times$ 10 nm). At negative sample bias, i.e., for tunneling out of occupied electronic states, the LDOS increases at -4 V, whereas at positive sample bias (unoccupied states), two structures are detected around 1.7 and 2.5 V. Between -4 and $+1.7$ V, the tunnel current remains finite and the dI/dU spectrum is essentially flat. The intensity of the LDOS peak around 1.7 V observed in STS for 1 ML MgO diminishes for 2 ML and is not detectable anymore for 3 ML (Fig. 2b). Therefore, we attribute this feature to MgO-Ag interface states [20]. In contrast, the high local density of unoccupied states around 2.5 eV does not decrease with film thickness and, consequently, is identified with MgO states [3,21]. From the UPS spectrum (Fig. 3a) of a 10 ML MgO film, which fixes the valence band maximum at about 4 eV below the Fermi level [22,23], and the EELS spectrum (Fig. 3b) of the same film, which shows the energy losses corresponding to the interband transitions in MgO bulk and at the MgO(001) surface of 7.8 eV (B) and

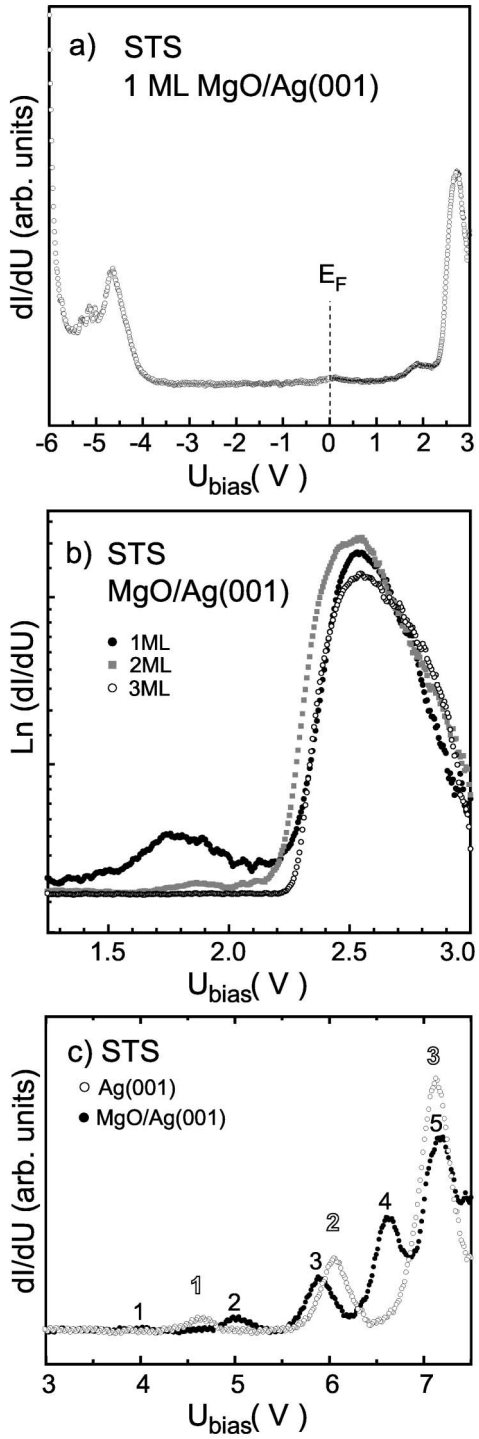

FIG. 2. STS of ultrathin MgO/Ag(001) films (U-sweep interval, tunneling parameters before opening the feedback loop, linear tip-sample distance variation): (a) tip placed above a 1 ML MgO island: -6.0 to 0 V, $U_0 = -6.0$ V, $I_0 = 0.2$ nA, $dz/dU = -0.12$ nm/V; 3.0 to 0 V, $U_0 = 3.0$ V, $I_0 = 0.2$ nA, $dz/dU = -0.16$ nm/V; (b) film thickness dependent dI/dU spectra: 3.0 to 1.0 V, $U_0 = 3.0$ V, $I_0 = 1.0$ nA, $dz/dU = -0.25$ nm/V; (c) Ag(001) field resonance states: ($\circ$) tip above Ag(001), ($\bullet$) tip above 1 ML MgO island; 7.5 to 3.0 V, $U_0 = 7.5$ V, $I_0 = 0.2$ nA, $dz/dU = -0.20$ nm/V.

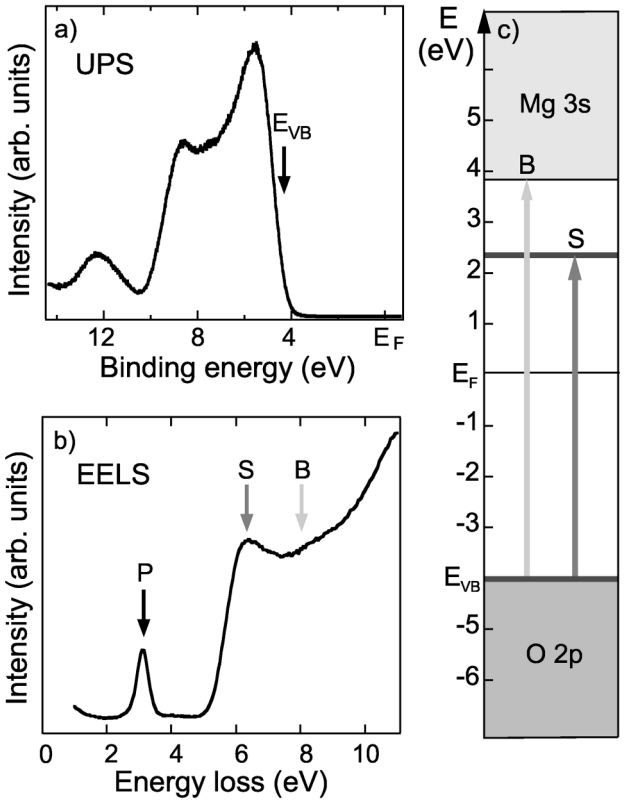

FIG. 3. Angle-resolved UPS and EELS of a 10 ML stoichiometric MgO(001)/Ag(001) film. (a) He II normal emission (E_{VB}: valence band onset). (b) EEL spectrum ($E_p = 30$ eV): Ag-MgO interface plasmon excitation (P) [17], lowest interband transition at the MgO(001) surface (S), bulk interband transition (B). (c) MgO(001) energy level scheme derived from (a) and (b).

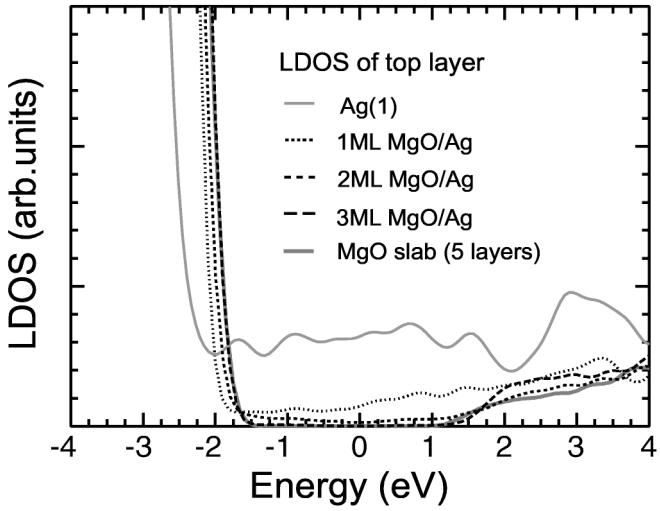

FIG. 4. Calculated surface layer LDOS for 0 to 3 MgO layers on a five-layer Ag-only slab and surface LDOS of a five-layer MgO-only slab (see text).

6.2 eV (S) [24–26], respectively, we deduce the energy level scheme illustrated in Fig. 3c. Thus, the onset of the 2.5 eV peak observed in STS (Figs. 2a and 2b) corresponds to the onset of the MgO(001) empty surface state band [24,27].

Combining STS (Figs. 2a and 2b) with conventional electron spectroscopy (Fig. 3), we conclude that the electronic structure of a MgO(001) single-crystal surface develops already within the first three monolayers.

We performed first principles calculations based on DFT to evaluate the layer-resolved LDOS as a function of the number n of adsorbed MgO layers ($0 \leq n \leq 3$) [28,29]. The calculated k-resolved LDOS for the 1 ML MgO system shows that screening of the Ag states by MgO is considerably more efficient at the surface Brillouin zone boundary than at Γ. Consequently, the states at Γ determine the minimum gap width, in agreement with the electronic structure of MgO [3,27,30]. In Fig. 4, we report the LDOS calculated in the plane of the first atomic layer in each system compared to a five-layer pure MgO slab. In the gap, the average surface LDOS decays exponentially with the number of adsorbed MgO layers. Increasing the MgO film thickness up to three layers produces a surface band gap corresponding to that of the five layer pure MgO slab, which is representative for the MgO(001) surface [31]. This result matches very well the experimental findings (Figs. 2a and 2b).

Differential conductance spectra above 3 V (Fig. 2c) show the first Ag(001) field resonance states (known as image states from two photon photoemission spectroscopy [32]) shifted towards higher energies caused by the electric field between the tip and sample [33]. When the tip is placed above a MgO island, these peaks shift towards lower energies consistent with the reduced work function (0.4 eV) observed in UPS for a 1 ML MgO/Ag(001) film. Field resonances may influence the apparent STM image contrast [34]. Thus their energetic positions can be used to distinguish between the oxide and the metal. In fact, in STM images taken at 5 V (Fig. 1a), which corresponds to the position of the second Ag(001) field resonance state when tunneling through 1 ML MgO (Fig. 2c), these islands appear clearly higher (0.30 nm vs 0.21 nm geometric height) than the Ag-Ag steps (0.20 nm). At higher coverage, when tunneling into MgO states, the apparent MgO-MgO step heights (Fig. 1d) correspond to their geometric heights.

At 2.5 V we obtain atomic resolution of the MgO layer (Fig. 1c). The lattice contains local defects and appears not perfectly arranged which may be due to the influence of the interface state on the image formation at the applied bias voltage. The observed surface lattice constant has twice the value of the one of MgO; thus only one type of ion is imaged. Within the gap (-4 to $+2.5$ V), the MgO reduces exponentially the probability of tunneling into the substrate. The remaining finite density of Ag states within the gap allows us to obtain atomic resolution

of the Ag(001) substrate imaged *through* a 1 ML MgO island (Fig. 1b) [35]. For bias voltages outside the gap, the islands appear always with bright contrast.

In summary, we found via STS investigations and model calculations that, within the first three atomic layers of MgO, a band gap of about 6 eV develops corresponding to the value for MgO(001) single crystals. By simply choosing accurately the number of dielectric spacer layers (1–3 ML), the electronic, magnetic, and chemical interaction between a metal substrate and atoms, molecules, clusters, or boundary layers adsorbed on the dielectric material may be tuned in a controlled manner. This opens new perspectives for the development of oxide heterostructure-based nanodevices [36] and applications in magnetoelectronics [37].

We thank K. Morgenstern for her contributions in the growth experiments and R. Berndt, H. Neddermeyer, and P. Varga for stimulating discussions. This work was supported by the Swiss National Science Foundation.

[1] J. S. Moodera *et al.,* Annu. Rev. Mater. Sci. **29**, 381–432 (1999).
[2] V. E. Henrich, Rep. Prog. Phys. **48**, 1481–1541 (1985).
[3] V. E. Henrich and P. A. Cox, in *The Surface Science of Metal Oxides* (Cambridge University Press, Cambridge, U.K., 1994).
[4] M. Bäumer *et al.,* in *Chemisorption and Reactivity on Supported Clusters,* edited by R. M. Lambert and G. Pacchioni (Kluwer Academic Publishers, Dordrecht, 1997).
[5] C. Xu and D. W. Goodman, in *Handbook of Heterogeneous Catalysis,* edited by G. Ertl, H. Knözinger, and J. Weitkamp (VCH, Weinheim, 1997), ISBN 3-527-29218-8.
[6] M. C. Gallagher *et al.,* Surf. Sci. **339**, L909 (1995).
[7] A. P. Alivisatos, Science **271**, 933 (1996).
[8] W. Hebenstreit *et al.,* Surf. Sci. Lett. **424**, L321 (1999).
[9] I. Sebastian *et al.,* Faraday Discuss. **144**, 129 (1999).
[10] J. Viernow *et al.,* Phys. Rev. B **59**, 10 356 (1999).
[11] R. Gaisch *et al.,* Ultramicroscopy **42–44**, 1621 (1992).
[12] J. Wollschläger *et al.,* Appl. Surf. Sci. **142**, 129 (1999).
[13] J. Tersoff and D. R. Hamann, Phys. Rev. B **31**, 805 (1985).
[14] R. M. Feenstra and P. Mårtensson, Phys. Rev. Lett. **61**, 447 (1988); P. Martensson and R. M. Feenstra, Phys. Rev. B **39**, 7744 (1989).
[15] W. J. Kaiser and R. C. Jaklevic, Surf. Sci. **181**, 55 (1987).
[16] In these modes band onsets naturally appear as peaks [10,14].
[17] M.-H. Schaffner *et al.,* Surf. Sci. **417**, 159 (1998).
[18] J. Li *et al.,* Phys. Rev. Lett. **76**, 1888 (1996).
[19] U. Heiz and W.-D. Schneider, J. Phys. D **33**, R85 (2000).
[20] S. Altieri *et al.,* Phys. Rev. B **61**, 16 948 (2000).
[21] A. L. Shluger *et al.,* Phys. Rev. B **59**, 2417 (1999).
[22] L. H. Tjeng *et al.,* Surf. Sci. **235**, 269 (1990).
[23] In photoemission as in STS the Fermi level is fixed by the metallic substrate. Tip-induced band bending is small as long as the LDOS of the metal substrate is "leaking" through the MgO film (Figs. 1 and 4b) [10,38].
[24] V. E. Henrich *et al.,* Phys. Rev. B **22**, 4764 (1980).
[25] P. A. Cox and A. A. Williams, Surf. Sci. **175**, L782 (1986).
[26] M.-C. Wu *et al.,* J. Vac. Sci. Technol. A **10**, 1467 (1992).
[27] U. Schönberger and F. Aryasetiawan, Phys. Rev. B **52**, 8788 (1995).
[28] The present results have been obtained using the ABINIT code (http://www.pcpm.ucl.ac.be/abinit).
[29] The Ag substrate is modeled by a five-layer slab separated by a vacuum layer (0.9–2.0 nm) with periodic boundary conditions. The O atoms of the first MgO layer are positioned on top of the Ag(001) surface atoms, which is the most favorable configuration [39–41]. We use a 288 k-point set to sample the surface Brillouin zone (SBZ), which reduces by symmetry to a set of 42 independent k points in the irreducible SBZ wedge. The calculated total energies of both the MgO and Ag bulk systems converge using a plane wave cutoff of 70 Ry. The pseudopotentials used to model the ionic cores [42] have been generated with the FHI98PP code [43] considering full ionic relaxation. For electronic exchange and correlation the generalized gradient approximation is used [44].
[30] J. P. LaFemina and C. B. Duke, J. Vac. Sci. Technol. A **9**, 1847 (1991).
[31] The absolute gap value is generally underestimated in the local density approximation [45], also found for MgO [39]. The surface electronic gap of the five-layer pure MgO slab, calculated here, is also underestimated (Fig. 4 [45]). The *difference* between the surface and bulk electronic gaps is, however, in good agreement with its experimental value (Fig. 3a [24–26]).
[32] S. Schuppler *et al.,* Appl. Phys. A **51**, 322 (1990).
[33] G. Binnig *et al.,* Phys. Rev. Lett. **55**, 991 (1985).
[34] For resonant tunneling into image states on metals see T. Jung *et al.,* Phys. Rev. Lett. **74**, 1641 (1995).
[35] This observation is expected when tunneling through an ultrathin insulator. An exponential decay of wave functions into the insulator completely agrees with the decay into an infinite insulator adjacent to a metal, as, e.g., into vacuum which is certainly not metallic.
[36] R. Chau *et al.,* in *Proceedings of IEEE International Electron Devices Meeting IEDM, 2000* (http://www.intel.com/research/silicon/ieee/ieee6.htm).
[37] G. A. Prinz, J. Magn. Magn. Mater. **200**, 57 (1999).
[38] M. McEllistrem *et al.,* Phys. Rev. Lett. **70**, 2471 (1993).
[39] U. Schönberger *et al.,* Acta Metall. Mater. **40**, 1–10 (1992).
[40] C. Li *et al.,* Phys. Rev. B **48**, 8317 (1993).
[41] E. Heifets *et al.,* J. Phys. Condens. Matter **8**, 6577 (1996).
[42] N. Troullier and J. L. Martins, Phys. Rev. B **43**, 1993 (1991).
[43] M. Fuchs and M. Scheffler, Comput. Phys. Commun. **119**, 67 (1999).
[44] J. P. Perdew *et al.,* Phys. Rev. Lett. **77**, 3865 (1996).
[45] See, e.g., W. Pickett, Comments Solid State Phys. **12**, 57 (1986), and references therein.